

Modeling the Global Levels and Distribution of Polychlorinated Biphenyls in Air under a Climate Change Scenario

LARA LAMON,^{†,‡} HARALD VON WALDOW,[§]
MATTHEW MACLEOD,^{*,§}
MARTIN SCHERINGER,[§]
ANTONIO MARCOMINI,^{†,‡} AND
KONRAD HUNGERBÜHLER[§]

CMCC, Euro-Mediterranean Centre for Climate Change,
Via Augusto Imperatore 16, 73100 Lecce, Italy, Department of
Environmental Sciences, University Ca' Foscari of Venice,
Calle Larga S. Marta 2137, 30123 Venice, Italy, and Safety and
Environmental Technology Group, Swiss Federal Institute of
Technology, Zürich, CH-8093, Switzerland

Received February 11, 2009. Revised manuscript received May 14, 2009. Accepted May 15, 2009.

We used the multimedia chemical fate model BETR Global to evaluate changes in the global distribution of two polychlorinated biphenyls, PCB 28 and PCB 153, under the influence of climate change. This was achieved by defining two climate scenarios based on results from a general circulation model, one scenario representing the last twenty years of the 20th century (20CE scenario) and another representing the global climate under the assumption of strong future greenhouse gas emissions (A2 scenario). The two climate scenarios are defined by four groups of environmental parameters: (1) temperature in the planetary boundary layer and the free atmosphere, (2) wind speeds and directions in the atmosphere, (3) current velocities and directions in the surface mixed layer of the oceans, and (4) rate and geographical pattern of precipitation. As a fifth parameter in our scenarios, we consider the effect of temperature on primary volatilization emissions of PCBs. Comparison of dynamic model results using environmental parameters from the 20CE scenario against historical long-term monitoring data of concentrations of PCB 28 and PCB 153 in air from 16 different sites shows satisfactory agreement between modeled and measured PCBs concentrations. The 20CE scenario and A2 scenario were compared using steady-state calculations and assuming the same source characteristics of PCBs. Temperature differences between the two scenarios is the dominant factor that determines the difference in PCB concentrations in air. The higher temperatures in the A2 scenario drive increased primary and secondary volatilization emissions of PCBs, and enhance transport from temperate regions to the Arctic. The largest relative increase in concentrations of both PCB congeners in air under the A2 scenario occurs in the high Arctic and the remote Pacific Ocean. Generally, higher wind speeds under the A2 scenario result in more efficient intercontinental transport of PCB 28 and PCB 153 compared

to the 20CE scenario. Our modeling indicates that, in a future impacted by climate change, we can expect increased volatilization emissions and increased mobility of persistent organic pollutants with properties similar to those of PCBs.

Introduction

The term “climate change” is defined by the Intergovernmental Panel on Climate Change (IPCC) as a change in the climate condition that can be identified by changes in the mean value or variability of a climate property that persist for an extended time, typically decades or longer (1). Evidence of climate change has been observed at both global and local scales. It includes changes in surface temperatures and ice cover in the Arctic, widespread changes in precipitation patterns and amounts, ocean salinity, wind patterns, and incidents of extreme weather, including droughts, heavy precipitation, heat waves, and intensity of tropical cyclones (2).

The scientific community has focused considerable attention on developing modeling tools to forecast global climate conditions. In 1980, the World Climate Research Programme (WCRP) was established with the goal to determine how predictable the climate is and to assess the effect of human activities on climate. The WCRP, together with the Program for Climate Model Diagnosis and Intercomparison (PCMDI), provides technical support for modeling studies initiated by the IPCC. Recently, climate model output from simulations of the past, present and future up to the year 2100 was collected by the PCMDI as the third phase of the Coupled Model Intercomparison Project (CMIP3). This collection of modeling results was used by the IPCC to prepare its Fourth Assessment Report and has been made publicly available to support scientific research into the potential effects of climate change.

Like climate change, environmental contamination by persistent organic pollutants (POPs) is an issue of global concern that is addressed by international agreements such as the Stockholm Convention (3). Researchers studying POPs have developed global-scale mass balance models that are appropriate for explaining differences in environmental fate and transport between chemicals and for exploring the influence of environmental parameters on the environmental fate of chemicals (4).

To date, only a few studies have examined interactions between climate change and the environmental distribution of POPs (5–10). Information that is available is mostly focused on the Arctic, a region of particular interest to scientists studying both global warming and contamination by POPs.

Here, we use the Berkeley–Trent global multimedia mass balance model (BETR Global) (8, 11), together with information from the WCRP CMIP3 multimodel data set, to model the fate of two archetypal POPs, PCB 28 and PCB 153, in the global environment. These substances were selected for this study because they are among the best characterized POPs in terms of physicochemical properties and emission estimates. We focus our attention on the atmosphere because atmospheric transport largely determines source-to-receptor relationships for POPs (12) and because PCB 28 and PCB 153 have been the subject of long-term monitoring programs that characterize concentrations in the atmosphere. We use these time-resolved emissions and measurement data to evaluate modeled concentrations of these chemicals against measurements for our base-case climate scenario, that is, the 20CE scenario as defined later in the paper.

* Corresponding author e-mail: macleod@chem.ethz.ch.

† CMCC, Euro-Mediterranean Centre for Climate Change.

‡ University Ca' Foscari of Venice.

§ Swiss Federal Institute of Technology.

The environmental behavior of PCBs and other persistent semivolatile substances depends on complex interactions between many factors within an open environmental system. Therefore, a comprehensive and predictive assessment of interactions between POPs and climate change is not technically feasible. Our approach to address this problem is to only consider a manageable subset of possible changes in climate conditions in our model scenarios and to systematically explore the effects of those changes on modeled concentrations in air. In particular, the climate scenarios used here are defined by differences in (1) temperature, (2) atmospheric circulation patterns, (3) ocean circulation patterns, and (4) precipitation rate. In addition, we also considered the effect of temperature differences between the climate scenarios on the rate of primary volatilization emissions of PCB 28 and PCB 153, since this has been identified as the dominant mechanism of release of PCBs to the atmosphere (13). We use steady state model experiments that assume a fixed source profile for PCBs to explore the interactions between these selected aspects of climate change and the major processes that govern the global distribution of these two substances.

Materials and Methods

Model and Parametrization. BETR Global has a spatial resolution of 15° latitude × 15° longitude or 288 grid cells that each define a model region. Each of these regions consists of up to 7 bulk compartments (ocean water, fresh water, planetary boundary layer (PBL), free atmosphere, soil, freshwater sediments, and vegetation). The model represents advective transport between the regions in air and water and intercompartment transport processes like dry and wet deposition and reversible partitioning (8). To model degradation of PCBs in the gas phase, the version of BETR Global applied in this study uses spatially and temporally resolved concentrations of OH radicals in the global atmosphere derived from Spivakovsky et al. (14).

BETR Global uses prescribed meteorological and oceanic data with a monthly time resolution. Precipitation rates, temperature fields and fluxes of air and ocean water across region boundaries are required as model inputs. In this project, these data were derived from the output of ECHAM5/MPI-OM (15), an atmosphere-ocean general circulation model (AOGCM). The data sets were obtained from the WCRP CMIP3 multimodel database, and are representative of the forecasts of the ensemble of models included in the IPCC's fourth Assessment Report (AR4) (16). To evaluate the influence of a climate change scenario on the environmental distribution of POPs, we use two different climate scenarios: one scenario representing current climatic conditions ("20CE") and one representing a possible future climate in the year 2100 ("A2").

Our 20CE scenario is based on the AOGCM output for the years 1981–2000 of the CMIP3 "Climate of the 20th Century Experiment" (20C3M). Our A2 scenario is based on the output for the years 2080 to 2099 of the CMIP3 "SRES A2 Experiment". The SRES (Special Report on Emission Scenarios) A2 scenario is the most extreme among the four "marker scenarios" that were considered in AR4 with respect to assumed cumulative greenhouse gas emissions and consequently also with respect to predicted temperature change until 2100 (1, 17).

From the AOGCM data sets, we calculated monthly averages over a 20-year period for (1) atmospheric temperature fields, (2) wind fields, (3) ocean current fields in the surface mixed layer, and (4) precipitation rates. These data sets were then regridded to match the spatial resolution of BETR Global, yielding a representative year of climatic conditions for each scenario that can be used to drive dynamic model calculations. The data were also averaged over the year to arrive at two steady state climate scenarios that can

be used in steady-state model calculations. The differences in these four environmental parameters between the two steady-state climate scenarios are illustrated in Figures S1–S5 in the Supporting Information (SI). In general, temperature in the planetary boundary layer is higher throughout the world under the A2 scenario, particularly in the Arctic. Wind speeds are also higher in the A2 scenario, particularly in the west-to-east direction at middle and high latitudes in both hemispheres. Ocean currents are faster in the west-to-east direction in the A2 scenario compared to the 20CE scenario, particularly at latitudes near the Antarctic and at high latitudes in the Northern Hemisphere in the Atlantic Ocean. Precipitation is higher under the A2 scenario, particularly in the Equatorial areas.

Physicochemical Properties and Emission Scenarios for PCB 28 and PCB 153. We used partitioning properties of PCB 28 and PCB 153 from Schenker et al. (18) and internal energies of phase change recommended by MacLeod et al. (19). Pseudo-first-order degradation half-lives in air were calculated from second-order hydroxyl radical reaction rate constants extrapolated from data presented by Anderson and Hites (20) and spatially and temporally resolved concentrations of OH radicals in the global atmosphere specified in the model; degradation half-lives in other compartments were estimated based on information in Wania and Daly (21) and the generic half-life classes recommended by Mackay et al. (22). These properties are shown in the SI in Table S1.

Breivik et al. (13) estimated the yearly global emissions of 22 PCB congeners for the period 1970–2100 using a mass balance approach that estimates production, use, disposal, and accidental spills of PCBs over their life-cycle. Because of the high uncertainties associated with these emission estimates, Breivik et al. presented "max", "default", and "min" emission estimates.

The information from Breivik et al. shows that the majority of primary PCB emissions to the atmosphere occur by passive volatilization from use and disposal of PCBs. This is important for our modeling study because, assuming that the strength of primary passive volatilization sources is proportional to vapor pressure of the PCB congener, source strength depends on temperature according to

$$\frac{E_2}{E_1} = \exp\left[\frac{\Delta U_A}{R} \times \left(\frac{1}{T_1} - \frac{1}{T_2}\right)\right] \quad (1)$$

where (E_2/E_1) is the ratio of the emission rates by passive volatilization at temperatures T_2 and T_1 , ΔU_A is the internal energy of vaporization of the PCB congener, and R is the gas constant. We applied eq 1 to model the intra-annual variability in PCB emissions in response to the seasonal cycle of temperature in our dynamic model runs. In addition, since temperature is one of the key variables in the two climate scenarios, we used eq 1 to estimate the increase in primary PCB emissions associated with increased temperature under the A2 scenario relative to the 20CE scenario. The rate of secondary revolatilization of PCBs from water, soils, and vegetation is also temperature dependent, but this is accounted for in the basic model structure of BETR Global.

Model Performance Evaluation. As a prerequisite to compare the fate of PCBs under the two climate scenarios, we first build confidence that our selected emission scenarios, physicochemical properties, and environmental fate model together provide a reasonable representation of PCBs in the global environment. To this end, we conduct dynamic model calculations to evaluate the performance of the model when it is run under the conditions of the 20CE scenario. We then perform steady-state calculations for two model experiments (described further below), in which we compare the 20CE and the A2 scenarios.

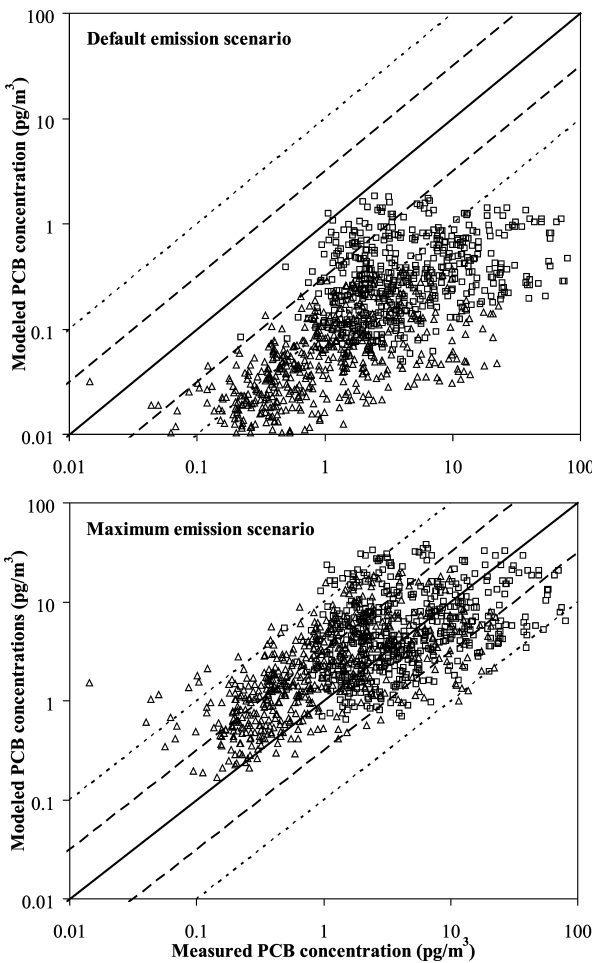


FIGURE 1. Comparison of seasonal averages of measured and modeled concentrations of PCB 28 (\square) and PCB 153 (\triangle) in air for the default and the maximum PCB emission estimates from Breivik et al. (13). Measurement data are from the 16 monitoring stations located in 9 different BETR regions and seasonal averages are for 3-month periods beginning in January. Diagonal lines indicate perfect agreement and agreement within factors of $10^{0.5}$ and 10.

To evaluate the model, we compare modeled concentrations of PCB 28 and PCB 153 under the 20CE climate scenario with PCB concentrations measured in air at 16 monitoring stations located in 9 different model regions (see Table S2, Supporting Information). Dynamic model results for the two PCB congeners were calculated for both the “max” and “default” emission scenarios from Breivik et al. (13) for the entire 170-year period from 1930–2100. This evaluation improves on the one reported earlier by MacLeod et al. (8) by (i) applying a new parametrization and new version of the model with improved treatment of degradation in the atmosphere and the intra-annual variability of primary volatilization emissions, and by (ii) considering more monitoring stations and additional monitoring data that has become available since the previous model evaluation.

Figure 1 compares modeled and measured seasonal (3-month) average concentrations of the two PCB congeners in air at the 16 monitoring stations for the two emission scenarios. Included in Figure 1 are data points for the period from 1990 to 2007, during which measured concentrations are available. Diagonal lines representing perfect agreement and agreement within factors of $10^{0.5}$ ($= 3.16$) and 10 are shown for comparison. Concentrations are clearly underpredicted with the default emission scenario. With the maximum emission scenario, 64% of the modeled concentrations are within a factor of 3.16 of the measured con-

centrations, and 96% are within 1 order of magnitude of the 1:1 line. We view this agreement between measured and modeled concentrations as satisfactory. Because the maximum emission scenario provides better agreement with field data, we use it in the steady state calculations to compare the two climate scenarios.

Figure S6 in the SI illustrates the same data as Figure 1 but as time series of modeled and measured concentrations of PCB 28 and PCB 153 at the different monitoring sites. At most sites, the model provides a reasonable description of the intra-annual variability and the inter-annual trends in the monitoring data.

Model Experiments. We performed two model experiments to compare the fate of PCB 28 and PCB 153 under the two climate scenarios. In the first experiment, we compare modeled concentrations of PCBs under the 20CE and A2 scenarios; then we parametrize several subscenarios based on the 20CE scenario, where we replace one of the five groups of parameters that differ between the two climate scenarios, that is, temperature, atmospheric circulation, oceanic circulation, precipitation, or emissions with parameter values from the A2 scenario. This first model experiment is designed to identify the effect of individual groups of environmental parameters on PCB distribution. In this experiment, we assumed a spatial distribution of PCB emissions corresponding to the maximum emission scenario.

The second experiment is performed to identify the effect of climate change on the distribution of PCBs released from different source regions. We consider five hypothetical emission scenarios in which North America, Europe, Asia, and South America, respectively, are the only primary source regions for PCBs, and we compare the results between the 20CE and A2 parametrizations of the model. Emissions are from the Great Lakes region and the United States northeast coast in our North America scenario, from central and eastern Europe in our European scenario, from the east coast of China and northern Japan in our Asia scenario and from southern Brazil in our South America scenario.

In both model experiments, we compute steady-state concentrations of PCB 28 and PCB 153 in the global environment, using annual average climate conditions. Volatilization sources of PCBs were distributed to each region according to total estimated emissions during the 170 year long maximum emission scenario estimated by Breivik et al. (13) and are the same in both climate scenarios. However, the emission rate to the atmosphere from these sources is adjusted for temperature as described above. To highlight the changes in levels and distribution attributable to differences in climate, these model experiments do not consider the large reductions in sources of PCBs that are expected to occur during the 21st century (13). Instead, we compare two alternative climate scenarios assuming that source characteristics of PCBs are the same in both scenarios and analyze our model results for the two PCB congeners in terms of global and hemispheric concentration levels and source-to-receptor relationships, with a focus on concentrations in the planetary boundary layer.

Results

Results of our model experiments are presented in Figures 2 (first experiment) and 3 (second experiment) as the ratio of concentration of PCBs in the planetary boundary layer in the A2 climate scenario to concentration in the 20CE scenario. Figures S8 and S9 in the Supporting Information show the same information as the difference in modeled concentrations in the planetary boundary layer between the 20CE and the A2 scenarios.

Figure 2A shows the ratio of modeled concentrations of PCBs at steady state in air in the planetary boundary layer under the A2 climate scenario to the concentrations under

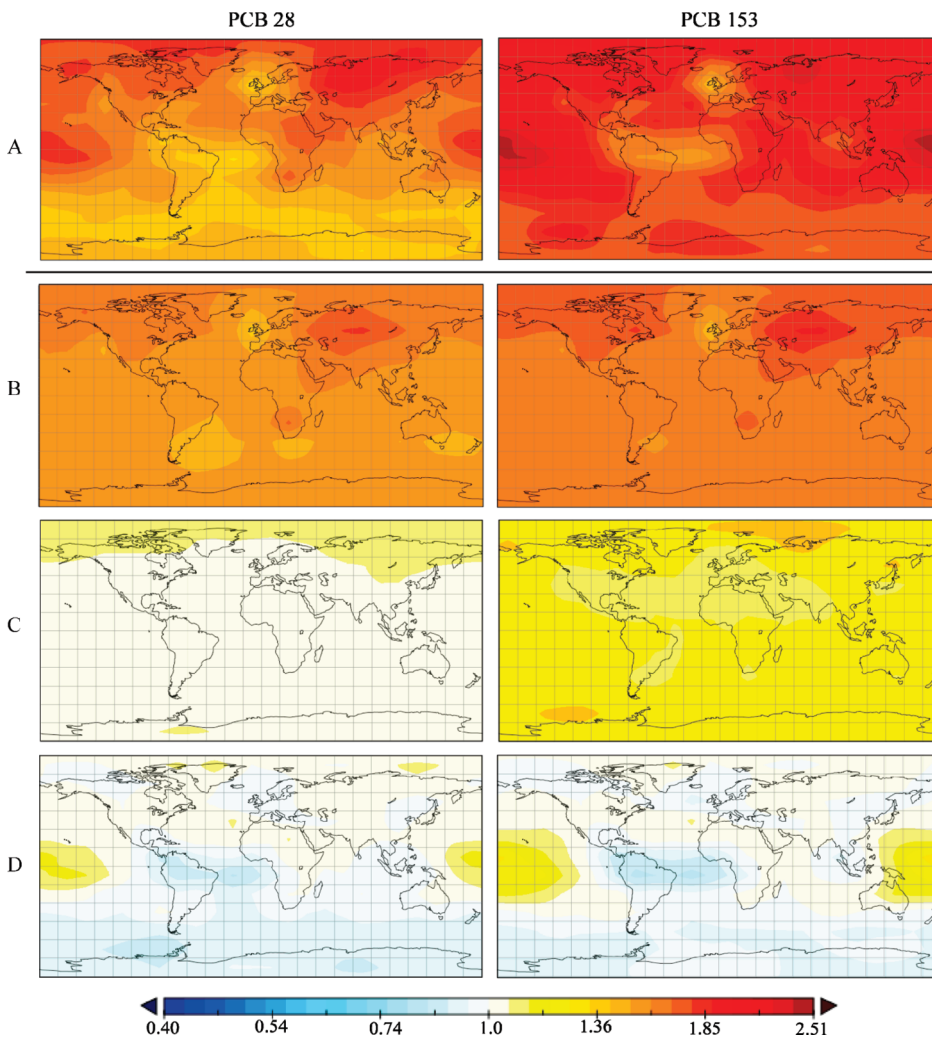


FIGURE 2. Ratio of modeled concentrations of PCBs at steady-state in the planetary boundary layer of the atmosphere under hypothetical climate conditions to modeled concentration under 20th century (20CE) conditions for PCB28 (left) and PCB153 (right). The hypothetical climate conditions are (A) the A2 climate change scenario, (B) the 20CE scenario with primary emission rates adjusted to reflect temperature in the A2 scenario, (C) temperature fields from the A2 scenario (excluding temperature influence on primary emissions), other parameters as in 20CE, and (D) wind fields from the A2 scenario, other parameters as in 20CE.

the 20CE scenario. For both congeners, concentrations in air are higher everywhere in the global atmosphere under the A2 scenario. The spatial pattern of increased concentrations is similar for PCB 28 and PCB 153 but the increase is more pronounced for PCB 153, up to a factor of 2.5, compared to a factor of 1.8 for PCB 28. Areas of notable increase in modeled concentrations are the Arctic and the equatorial Pacific Ocean.

The other panels of Figure 2 show results from the first model experiment, where we constructed hypothetical climate scenarios from one climate parameter taken from the A2 climate scenario and all other parameters from the 20CE scenario. Shown are the three parameters with the strongest influence on the concentration patterns in air. These are temperature effects on emissions (panel B), temperature effects on dynamic repartitioning and degradation (panel C) and wind speeds (panel D). The other two environmental parameters, oceanic currents and precipitation, lead to much smaller changes in environmental behavior of PCBs in lower air (Figure S7 in the SI).

Figure 2 shows that different parameters contribute to the overall difference between the A2 and 20CE scenarios at different locations. The effect of temperature on primary emissions (Figure 2B) results in a general increase in concentrations throughout the globe that is stronger for PCB 153 than for PCB 28. This increase is strongest over central

Asia, which is caused by increased primary volatilization emissions in eastern Europe and Russia. The effect of higher temperatures under the A2 scenario on environmental partitioning and degradation of PCBs results in higher concentrations globally, especially in the Arctic and, to a lesser extent, the Antarctic (Figure 2C). The changes in atmospheric circulation patterns account for higher concentrations of both congeners in the equatorial Pacific, and lower concentrations in the equatorial Atlantic and over Antarctica (Figure 2D).

Figure 3 shows results for our second model experiment, in which the A2 climate scenario is compared to the 20CE scenario for emissions only in North America, Europe, Asia, and South America. For PCB 28, regardless of emission location, the modeled concentrations in air in the hemisphere where emissions occur increase, and there is a slight decrease in the other hemisphere, reflecting that the average half-life of PCB 28 in air is not long enough for efficient interhemispheric mixing. Furthermore, modeled concentrations of PCB 28 are higher in the direction “downwind” (i.e., eastward) of the source regions under the A2 scenario, and are in some cases lower immediately “upwind” (i.e., westward). This trend implies an increased potential for intercontinental transport and transport into the Arctic and is most obvious for emissions in Europe, but is also apparent for emissions in North America and Asia. For PCB 153, modeled concentra-

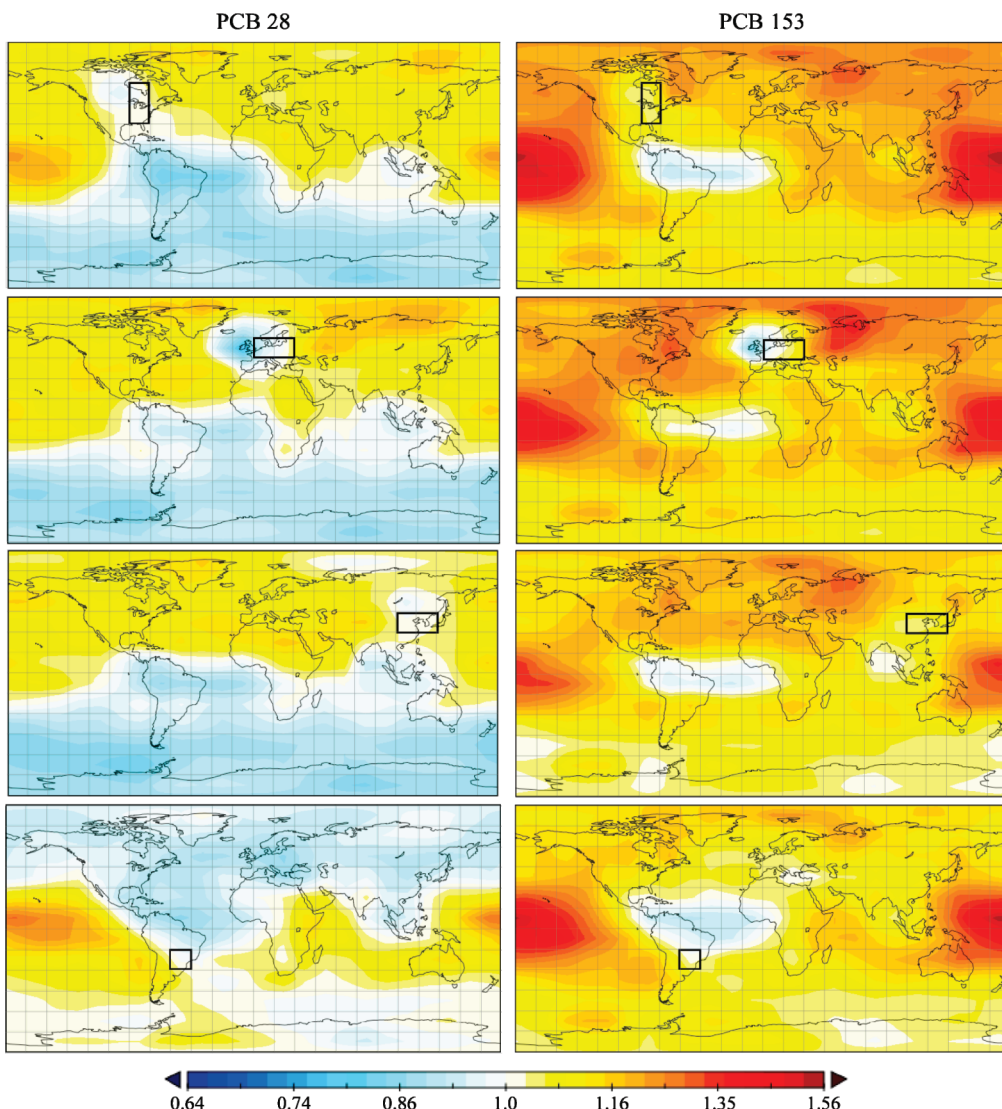


FIGURE 3. Ratio of modeled PCB concentration at steady-state in the planetary boundary layer of the atmosphere under the A2 climate scenario to modeled concentration under the 20CE scenario for PCB28 (left) and PCB 153 (right) for emission in North America, Europe, Asia, and South America (top to bottom).

tions in air increase in both hemispheres under the A2 scenario compared to the 20CE scenario. The pattern of higher concentrations downwind from source regions under the A2 scenario is again evident, implying increased intercontinental transport and transport to the Arctic. In all scenarios, the modeled PCB concentrations in equatorial regions over the Pacific Ocean are higher under the A2 scenario than under the 20CE scenario.

Discussion

First, we report a model evaluation of BETR Global in which modeled concentrations for PCB 28 and PCB 153 are compared to field data. The agreement between measured and modeled concentrations (Figure 1 and SI Figure S6) demonstrates that, under the 20CE scenario, the model can account for much of the variability in monitoring data between sites and over time. In the model evaluation, we used the dynamic version of the model, whereas we examined the effect of the climate change scenario using steady-state calculations. Dynamic calculations were used to evaluate the model against recent monitoring data because PCBs are not currently near steady-state in the global environment. However, steady-state concentrations were selected to

evaluate the effect of the A2 climate scenario because they reflect the long time-scale associated with POPs, and the steady-state concentration is a surrogate for cumulative environmental exposure, regardless of the temporal pattern of emissions (23). Therefore, our modeling does not predict concentrations of contaminants in the atmosphere in the future but rather analyzes changes under a climate change scenario relative to a base case scenario.

Second, results from our first model experiment identified temperature and atmospheric circulation patterns as the climate parameters affecting the PCB distribution in the planetary boundary layer most strongly. The increase of primary volatilization emissions as a result of higher temperature in the A2 scenario is the single most influential effect of climate change on the modeled concentrations of both PCB 28 and PCB 153 in air. The effect of increased temperature on the strength of primary volatilization emissions of POPs has not been explicitly characterized in earlier modeling studies (5, 6, 8), which focused on the impact of changes in atmospheric circulation, rainfall, and the effect of temperature on secondary re-emission from soils and vegetation. However, our results demonstrate that the more efficient mobilization of POP-like substances from primary

sources in a future impacted by global-scale warming may dominate all other effects of climate change on global-scale pollutant dynamics. The larger absolute value of the internal energy of vaporization (ΔU_A) of PCB 153 (91.6 kJ/mol) relative to PCB 28 (77.6 kJ/mol) accounts for the stronger effect of temperature on emissions of PCB 153.

Third, the results in Figure 2C demonstrate that higher temperatures in the A2 scenario result in higher modeled concentrations of both PCB congeners in air, even when emissions are held constant. This is the net result of two competing parameters: (i) increased volatilization from secondary sources, which is determined by ΔU_A , and (ii) increased degradation in surface media, which is determined by the assumed activation energies for degrading reactions (30 kJ/mol for all compartments except the atmosphere, where the degradation rate constant is only a function of hydroxyl radical concentrations). Modeled concentrations in air resulting from secondary volatilization are higher in the warmer A2 scenario because volatilization rate is more temperature dependent than degrading reactions in surface media. However, the overall persistence in the multimedia environment is lower under the A2 scenario (PCB 28, 2.7 years in the A2 scenario versus 3.8 years in the 20CE scenario; PCB 153, 8.7 years versus 10.9 years). Therefore, our model results suggest that substances with properties similar to those of PCBs are less persistent in the environment, but more efficiently transported in the global atmosphere under the A2 scenario compared to the 20CE scenario.

Shindell et al. (24) used results from a global circulation model to argue that a future impacted by anthropogenic climate change would be characterized by a persistent shift toward positive values of the North Atlantic Oscillation (NAO) index. Two earlier modeling studies have used historical data to examine relationships between positive NAO index and global-scale pollutant transport in the atmosphere (8, 24). Both of these studies found increased transport of pollutants to the Arctic under positive NAO conditions. Our findings are consistent with these earlier studies in that our modeled transport of PCBs to the Arctic is higher in the A2 climate change scenario. In addition, our finding that transport of pollutants from European sources to the Arctic is more enhanced in the A2 scenario than transport from sources in North America or Asia is consistent with the results reported by Eckhardt et al. (25).

The model results presented here provide some initial estimates of the possible effects of climate change on the environmental distribution of POPs, and our effort can be considered as a first step in answering the questions put forward by the UNECE (26) on this topic. Overall, our model assessment forecasts that under the influence of climate change the world may, in effect, "become smaller", that is, enhanced volatilization emissions of POPs can be expected to be more efficiently transported across national boundaries and into remote areas. However, it should be recognized that this work is not a comprehensive assessment. We considered only four environmental parameters in our climate scenarios, and these do not cover the full spectrum of phenomena that may result from climate change.

Acknowledgments

We acknowledge the modeling groups, the Program for Climate Model Diagnosis and Intercomparison (PCMDI) and the WCRP's Working Group on Coupled Modeling (WGCM) for their roles in making available the WCRP CMIP3 multimodel data set. Support of this data set is provided by the Office of Science, U.S. Department of Energy. We gratefully acknowledge the Euro-Mediterranean Centre for Climate Change (CMCC; Lecce, Italy) for financial support.

Supporting Information Available

Figures illustrating the differences in environmental parameterizations of the BETR Global model for the 20CE and A2 climate scenarios, physicochemical property data for PCB 28 and PCB 153 used in our calculations, figures comparing the time series of modeled and measured concentrations of PCB 28 and PCB 153 at long-term monitoring sites, continuation of Figure 2 illustrating the ratio of modeled concentrations, when only ocean circulation pattern and only precipitation from the A2 scenario are considered. This material is available free of charge via the Internet at <http://pubs.acs.org>.

Note Added after ASAP Publication

The affiliations have been modified in the version of this paper published ASAP June 22, 2009; the corrected version published ASAP July 1, 2009.

Literature Cited

- (1) Bernstein, L.; Bosch, P.; Canziani, O.; Chen, Z.; Christ, R.; Davidson, O.; Hare, W.; Huq, S.; Karoly, D.; Kattsov, V.; Kundzewicz, Z.; Liu, J.; Lohmann, U.; Manning, M.; Matsuno, T.; Menne, B.; Metz, B.; Mirza, M.; Nicholls, N.; Nurse, L.; Pachauri, R.; Palutikof, J.; Parry, M.; Qin, D.; Ravindranath, N.; Reisinger, A.; Ren, J.; Riahi, K.; Rosenzweig, C.; Rusticucci, M.; Schneider, S.; Sokona, Y.; Solomon, S.; Stott, P.; Stouffer, R.; Sugiyama, T.; Swart, R.; Tirpak, D.; Vogel, C.; Yohe, G. *Climate Change 2007: Synthesis Report*, 2008. http://www.ipcc.ch/pdf/assessment-report/ar4/syr/ar4_syr.pdf.
- (2) Trenberth, K. E.; Jones, P. D.; Ambenje, P.; Bojariu, R.; Easterling, D.; Klein, T. A.; Parker, D.; Rahimzadeh, F.; Renwick, J. A.; Rusticucci, M.; Soden, B.; and Zhai, P. *Climate Change 2007: The Physical Science Basis*, 2007. <http://www.ipcc.ch/pdf/assessment-report/ar4/wg1/ar4-wg1-chapter3.pdf>.
- (3) UNEP, Stockholm Convention on Persistent Organic Pollutants, 2004. <http://www.pops.int>.
- (4) McKone, T. E.; MacLeod, M. Tracking multiple pathways of human exposure to persistent multimedia pollutants: Regional, continental, and global-scale models. *Annu. Rev. Environ. Resour.* **2003**, *28*, 463–492.
- (5) McKone, T. E.; Daniels, J. I.; Goldman, M. Uncertainties in the link between global climate change and predicted health risks from pollution: Hexachlorobenzene case study using a fugacity model. *Risk Anal.* **1996**, *16*, 377–393.
- (6) Dalla Valle, M.; Marcomini, A.; Codato, E. Climate change influence on POPs distribution and fate: A case study. *Chemosphere* **2007**, *67*, 1287–1295.
- (7) Macdonald, R. W.; Harner, T.; Fyfe, J. Recent climate change in the Arctic and its impact on contaminant pathways and interpretation of temporal trend data. *Sci. Total Environ.* **2005**, *342*, 5–86.
- (8) MacLeod, M.; Riley, W. J.; McKone, T. E. Assessing the influence of climate variability on atmospheric concentrations of polychlorinated biphenyls using a global-scale mass balance model (BETR-Global). *Environ. Sci. Technol.* **2005**, *39*, 6749–6756.
- (9) Ma, J.; Hung, H.; Blanchard, P. How do climate fluctuations affect persistent organic pollutant distribution in North America? Evidence from a decade of air monitoring. *Environ. Sci. Technol.* **2004**, *38*, 2538–2543.
- (10) Becker, S.; Halsall, C. J.; Tych, W.; Kallenborn, R.; Su, Y.; Hung, H. Long-term trends in atmospheric concentrations of α - and γ -HCH in the Arctic provide insight into the effects of legislation and climatic fluctuations on contaminant levels. *Atmos. Environ.* **2008**, *42*, 8225–8233.
- (11) MacLeod, M.; Woodfine, D. G.; Mackay, D.; McKone, T. E.; Bennett, D.; Maddalena, R. BETR North America: A regionally segmented multimedia contaminant fate model for North America. *Environ. Sci. Pollut. Res.* **2001**, *8*, 156–163.
- (12) Stroebe, M.; Scherer, M.; Held, H.; Hungerbühler, K. Intercomparison of multimedia modeling approaches: Modes of transport measures of long range transport potential and the spatial remote state. *Sci. Total Environ.* **2004**, *321*, 1–20.
- (13) Breivik, K.; Sweetman, A.; Pacyna, M. J.; Jones, K. C. Towards a global historical emission inventory for selected PCB congeners—A mass balance approach 3. An update. *Sci. Total Environ.* **2007**, *377*, 296–307.
- (14) Spivakovskiy, C. M.; Logan, J. A.; Montzka, S. A.; Balkanski, Y. J.; Foreman-Fowler, M.; Jones, D. B. A.; Horowitz, L. W.; Fusco,

- A. C.; Brenninkmeijer, C. A. M.; Prather, M. J.; Wofsy, S. C.; McElroy, M. B. Three-dimensional climatological distribution of tropospheric OH: Update and evaluation. *J. Geophys. Res.* **2000**, *105*, 8931–8980.
- (15) Roeckner, E.; Bäuml, G.; Bonaventura, L.; Brokopf, R.; Esch, M.; Giorgetta, M.; Hagemann, S.; Kirchner, I.; Kornblueh, L.; Manzini, E.; Rhodin, A.; Schlese, U.; Schulzweida, U.; Tompkins, A. *The Atmospheric General Circulation Model ECHAM 5. Part I: Model Description*. MPI Report 349; Max Planck Institute for Meteorology: Hamburg, Germany, 2003; http://www.mpimet.mpg.de/fileadmin/publikationen/Reports/max_scirep_349.pdf.
- (16) Meehl, G. A.; Covey, C.; Delworth, T.; Latif, M.; McAvaney, B.; Mitchell, J. F. B.; Stouffer, R. J.; Taylor, K. E. The WCRP CMIP3 multimodel dataset: A new era in climate change research. *Bul. Am. Meteorol. Soc.* **2007**, *88*, 1383–1394.
- (17) Nakicenovic, N.; Alcamo, J.; Davis, G.; de Vries, B.; Fenmann, J.; Gaffin, S.; Gregory, K.; Grubler, A.; Jung, T.; Kram, T.; La, E.; Michaelis, L.; Mori, S.; Morita, L.; Pepper, W.; Pitcher, H. M.; Price, L.; Riahi, K.; Roehrl, A.; Rogner, H.; Sankovski, A.; Schlesinger, M.; Shukla, P.; Smith, S. J.; Swart, R.; van Rooijen, S.; Victor, N.; Dadi, Z. IPCC Special Report on Emissions Scenarios, 2000. http://www.grida.no/publications/other/ipcc_sr/?src=/climate/ipcc/emission/.
- (18) Schenker, U.; MacLeod, M.; Scheringer, M.; Hungerbühler, K. Improving data quality for environmental fate models: A least-squares adjustment procedure for harmonizing physicochemical properties of organic compounds. *Environ. Sci. Technol.* **2005**, *39*, 8434–8441.
- (19) MacLeod, M.; Scheringer, M.; Hungerbühler, K. Estimating enthalpy of vaporization from vapor pressure using Trouton's rule. *Environ. Sci. Technol.* **2007**, *41* (8), 2827–2832.
- (20) Anderson, P. N.; Hites, R. A. OH radical reactions: The major removal pathway for polychlorinated biphenyls from the atmosphere. *Environ. Sci. Technol.* **1996**, *30*, 1756–1763.
- (21) Wania, F.; Daly, G. L. Estimating the contribution of degradation in air and deposition to the deep sea to the global loss of PCBs. *Atmos. Environ.* **2002**, *36*, 5581–5593.
- (22) Mackay, D.; Shiu, W. Y.; Ma, K. C.; Lee, S. C. *Handbook of Physical-Chemical Properties and Environmental Fate for Organic Chemicals*, 2nd ed.; CRC: Boca Raton, FL, 2006.
- (23) von Waldow, H.; Scheringer, M.; Hungerbühler, K. Modeled environmental exposure to contaminants is independent of the time course of emissions: Proof and significance for chemical assessment, exposure. *Ecol. Modell.* **2008**, *219*, 256–259.
- (24) Shindell, D. T.; Miller, R. L.; Schmidt, G. A.; Pandolfi, L. Simulation of recent northern winter climate trends by greenhouse-gas forcing. *Nature* **1999**, *399*, 452–455.
- (25) Eckhardt, S.; Stohl, A.; Beirle, S.; Spichtinger, N.; James, P.; Forster, C.; Junker, C.; Wagner, T.; Platt, U.; Jennings, S. G. The North Atlantic Oscillation controls air pollution transport to the Arctic. *Atmos. Chem. Phys.* **2003**, *3*, 1769–1778.
- (26) UNECE. Report of the executive body on its twenty-fifth Session held in Geneva from 10 to 13 December, 2007. <http://www.unece.org/env/documents/2007/eb/EB/ece.eb.air.91.add.2.Amend.1.e.pdf>.

ES900438J